

Mass measurement in boosted decay systems at hadron colliders

Won Sang Cho^a, William Klemm^{a,b}, and Mihoko M. Nojiri^{a,c,d}

^a *Institute for the Physics and Mathematics of the Universe, University of Tokyo, Chiba 277-8582, Japan*

^b *Department of Physics, University of California, Berkeley, California 94720, USA*

^c *Theory Group, KEK, 1-1 Oho, Tsukuba, Ibaraki 305-0801, Japan and*

^d *The Graduate University for Advanced Studies (SOKENDAI), 1-1 Oho, Tsukuba, Ibaraki 305-0801, Japan*

We report a new possibility of using the M_{CT2} (Constransverse mass) variable for mass measurement in single step decay chains involving missing particles with moderate transverse momentum. We show that its experimental feasibility is enhanced compared to the corresponding M_{T2} -kink method. We apply this method to reconstruct a pair of chargino decay chains.

PACS numbers: 12.60.Jv, 13.85.Hd, 14.80.Ly, 13.90.+i

Many theories of new physics beyond the Standard Model (SM) are expected to provide a rich invisible energy signal from their Lightest New Particles (LNP), which are stable Dark Matter candidates, missing in the detector of future hadron colliders. In this situation only the so-called ‘ M_{T2} -kink’ method can provide the information necessary to determine the masses of both mother particle and missing LNP simultaneously for the events with a pair of single step decay chains [1, 2].

The origin of the M_{T2} -kink is the variety of ‘Extreme Kinematic Configurations (EKCs)’ in the events which can contribute to the maximum of the M_{T2} distribution. In general, for a given trial LNP mass, χ , the different EKC’s will take on different values, so in different regions of χ , $M_{T2}^{\max}(\chi)$ will follow different functional forms. At the true value, $\chi = m_X$, all of the EKC should provide the same M_{T2} maximum value as the true mother particle mass, m_Y , by the definition of M_{T2} [3]. Consequently, $M_{T2}^{\max}(\chi)$ shows a slope discontinuity at the kink point, $M_{T2}^{\max}(\chi = m_X) = m_Y$.

Let us consider the system of a pair of single step decay chains at the LHC: $p + p \rightarrow \delta_T + Y_1/Y_2 (\rightarrow \alpha X_1/\beta X_2)$, where $Y_{1,2}$ are the two mother particles with identical masses, each decaying to visible $\alpha(\beta)$ and missing LNP ($X_{1(2)}$). δ_T denotes the other remnants (and the sum of their transverse momenta) not from Y_i decays, i.e. from the Initial State Radiation (ISR) or decays before Y_i , so that they provide the total transverse momentum of the Y_{1+2} system of $-\delta_T$. In this event topology, there are two physical degrees of freedom that can generate the variety of EKC developing the kink. One is the invariant mass of visible particles $m_{\alpha,\beta}$ in $N(\geq 3)$ -body decays, generating a so-called ‘Mass Kink’ [1], and the other one is non-zero transverse momentum (δ_T) leading to a ‘Boosted Kink (BK)’ [2] of the Y_{1+2} system of our interest. When $\alpha(\beta)$ consists of a single visible particle and has a fixed invariant mass, then only the BK provides enough constraints for simultaneous mass measurement.

However, the BK is not easy to identify [2]. It requires large δ_T to have a clear kink structure. With the highest practical values of $\delta_T/m_Y \sim O(1-10)$ at the LHC, the kink structure is not clear enough to be reliably measured. The profile of the δ_T distribution is sharply decreasing for large values at the LHC, and the endpoint

structure of the $M_{T2}(\chi)$ distribution is smeared for large δ_T with small statistics. This can introduce significant systematic errors in the endpoint extractions.

In this paper we present the endpoint behavior of the $M_{CT2}(\chi)$ distribution [4] for single step decay chains with non-zero δ_T . The $M_{CT2}^{\max}(\chi)$ distributions for different δ_T carry independent information about m_Y and m_X , and it can be utilized for simultaneous mass measurement of mother and missing particles. Furthermore, as the dependence of M_{CT2} on δ_T is much more significant compared with the M_{T2} , it becomes good collider basis in resolving the boundary of the distorted phase space by various transverse boost effects. One more interesting property is that the endpoint structure is statistically cleaner with much less pollution from unwanted width effect in addition to the amplification and sharpening of the structure as noticed in [4]. In next sections, we describe the merit of using M_{CT2}^{\max} over M_{T2}^{\max} for systems in which reasonable δ_T is expected from heavy colored NP particle decays. We demonstrate that it can be used to probe the boosted kinetic boundary, and determine the masses of the particles involved in the chargino decays into sleptons, in particular $\tilde{\chi}_1^\pm \rightarrow \tilde{\nu} (\rightarrow \tilde{\chi}_1^0 + \nu) + \ell$.

The M_{CT2} (Constransverse mass) variable [4] for the Y_{1+2} system is defined by replacing M_T with M_{CT} [5] in the definition of M_{T2} [3] as follows:

$$M_{CT2}(\chi) = \min_{k_{1T}+k_{2T}=\cancel{E}_T} \left[\max \{M_{CT}^{(1)}, M_{CT}^{(2)}\} \right] \quad (1)$$

$$M_{CT}^{(1)}(\chi)^2 = \chi^2 + 2(|\alpha_T|e_1 + \alpha_T \cdot k_{1T}),$$

where $M_{CT}^{(2)}(\chi)$ is defined by replacing (α_T, e_1, k_{1T}) with (β_T, e_2, k_{2T}) . $k_{1,2T}$ and $e_{1,2}$ are the transverse (Tr) momenta and Tr energy, respectively, of missing $X_{1,2}$, with total missing Tr momentum, $\cancel{E}_T = -(\alpha_T + \beta_T) - \delta_T$. $\alpha_T(\beta_T)$ represents the Tr momenta of visible particles from $Y_1(Y_2)$ decays, $-\delta_T$ is the total Tr momentum of the Y_{1+2} system, and χ denotes the trial test mass of X_i . Visible particle masses are assumed to be zero, however the definition of M_{CT2} can be easily generalized for massive visible particle events. In [4], it was found that the number of events near M_{CT2}^{\max} can be amplified with a judicious choice of trial mass, χ , and M_{CT2} was employed to measure some physical constraints involving squark and

gluino masses with fewer systematic errors in pinpointing the endpoint than with the M_{T2} analysis. One thing worthy to note here is that interestingly, the endpoint of the $M_{T2}(\chi)$ [1, 2] or $M_{CT2}(\chi)$ [4] for any χ values, is invariant under the unknown $\sqrt{s}(\geq 2m_Y)$ values of the system with two mother particles, and this property is also satisfied by the $M_{CT2}^{\max}(\chi)$ for general boosted decay system as in following paragraphs.

When $\delta_T = 0$, the $M_{CT2}(\chi)$ has a one-to-one correspondence with $M_{T2}(\chi)$, and its maximum value is given as follows [4] :

$$M_{CT2}^{\max 2}(\chi) = \chi^2 + 2(\alpha_0 E_X^0 - \alpha_0^2), \quad (2)$$

where $\alpha_0 = \frac{m_Y^2 - m_X^2}{2m_Y}$ and $E_X^0 = \sqrt{\chi^2 + \alpha_0^2}$. However, if $\delta_T \neq 0$, simple one-to-one correspondence no longer exists, except for the events of some EKC. Certainly, depending on χ , $M_{CT2}(\chi)$ and $M_{T2}(\chi)$ can be one-to-one, however, it's not valid in general χ values. In result, the maximum profile of the $M_{CT2}(\chi)$ distribution shows a 2nd order Boosted Kink, (${}^2\text{BK}$), structure which is different from the BK of M_{T2} . As investigated in [1, 2], the $M_{T2}^{\max}(\chi, \delta_T)$ value of the Y_{1+2} system is the same as the $M_T^{\max}(\chi, \delta_T/2)$ of single Y_i decay system, and the EKC for the M_{T2}^{\max} can be characterized by a pair of identical EKC's corresponding to the M_T^{\max} of single Y_i decays although they have to be combined to produce the event with general $\sqrt{s} \geq 2m_Y$. Then, in the language of single Y_i decay, the BK of $M_{T2}^{\max}(\chi)$ is provided by two EKC's of the single Y_i decay events, characterized as follows :

$$\text{a) } \phi^{\max} = 0 \text{ for } \chi \leq m_X \quad \text{b) } \phi^{\max} = \pi \text{ for } \chi \geq m_X$$

where ϕ^{\max} is the azimuthal angle between visible Tr momentum and δ_T in the rest frame of the Y_i with vanishing $\Delta\eta(\equiv \eta_{vis} - \eta_{inv})$. Similarly, the EKC's for $M_{CT2}^{\max}(\chi)$ with ${}^2\text{BK}$ can be also characterized by single Y_i decays, but the azimuthal angle dependence is different :

$$1) \cos \phi^{\max} = \frac{m_X^2 m_Y^2}{|\delta_T| E_Y (m_Y^2 - m_X^2)} \left[\frac{\chi^2}{m_X^2} + \frac{|\delta_T|^2}{m_Y^2} \right] \text{ for } \chi \leq \chi_*$$

$$2) \cos \phi^{\max} = -1 \text{ for } \chi \geq \chi_*,$$

where $|\bar{\delta}_T| = |\delta_T|/2$ and $E_Y = \sqrt{m_Y^2 + |\bar{\delta}_T|^2}$. Thus, $M_{CT2}^{\max}(\chi)$ is described by two curves in the two regions of χ divided at χ_* , where χ_* is given by

$$\chi_*^2 = |\bar{\delta}_T| (2\alpha - |\bar{\delta}_T|), \quad (3)$$

with $\alpha = |\alpha_0| \left(\frac{|\delta_T|}{m_Y} + \frac{E_Y}{m_Y} \right)$. Then M_{CT2}^{\max} for the full χ range is given as follows :

$$M_{CT2}^{\max 2} = 2\chi^2 + |\bar{\delta}_T|^2 \quad \text{for } \chi \leq \chi_* \quad (4)$$

$$= \chi^2 + 2\alpha(|\bar{\delta}_T| - \alpha) + 2\alpha\sqrt{\chi^2 + (|\bar{\delta}_T| - \alpha)^2} \quad \text{for } \chi \geq \chi_*. \quad (5)$$

When χ_* is real, the two maximal curves of Eq. (4) and (5) come into contact at χ_* with the same inclination,

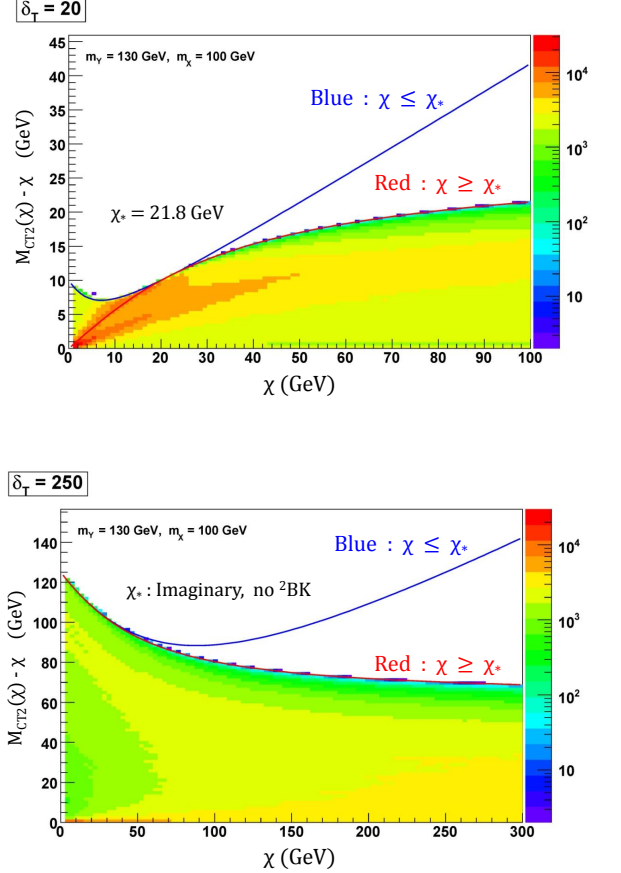


FIG. 1: a) $M_{CT2}^{\max}(\chi)$ for $(m_Y, m_X) = (130, 100)$ GeV and $\delta_T^* = 247.9$ GeV with $\delta_T = 20$ GeV ($\chi_* = 21.8$ GeV) b) $M_{CT2}(\chi)$ distribution for $\delta_T = 250$ GeV (No ${}^2\text{BK}$).

but the curvature of $M_{CT2}^{\max}(\chi)$ has a discontinuity at $\chi = \chi_*$ which we denote ${}^2\text{BK}$. It's interesting that when a ${}^2\text{BK}$ exists, there is a boost-trapped distribution for $\chi < \chi_*$ in that its boundary is independent of any physical masses in the decay system, as shown in Eq. (4). If χ_* is imaginary, $M_{CT2}^{\max}(\chi \geq 0)$ just follows the line given by Eq. (5). For given parameters, $(m_Y, m_X, |\delta_T|)$, χ_* is real and observable if

1. $\frac{m_X}{m_Y} \leq \frac{1}{\sqrt{2}}$, then $\chi_* \in \mathbf{R}$.
2. $\frac{1}{\sqrt{2}} < \frac{m_X}{m_Y} < 1$, then $\chi_* \in \mathbf{R}$ if $|\delta_T| \leq |\delta_T^*|$,
where $|\delta_T^*| \equiv 4\alpha_0 / \sqrt{1 - \frac{4\alpha_0}{m_Y}}$.

The reality condition of χ_* for the existence of a ${}^2\text{BK}$ is not always met, however, it certainly appears for the events with small values of $|\delta_T|$. For example, Fig. (1) shows contour histogramming on the $M_{CT2}(\chi) - \chi$ vs χ plane. We used the 10^5 Monte-Carlo events which simulate the phase space of the pair of boosted decay system, $Y_{1+2} + \delta_T$ where $(m_Y, m_X, \delta_T) = (130, 100, 20)$ GeV with massless visible particle. In Fig. (1(a)) the $M_{CT2}^{\max}(\chi)$ is well described by the two curves in the two regions

of χ divided by ${}^2\text{BK}$, $\chi_* = 21.8 \text{ GeV}$. For $\chi \leq \chi_*$, $M_{CT2}^{\text{max}}(\chi)$ follows the blue curve; it switches to the red one for $\chi \geq \chi_*$ with a continuous slope at $\chi = \chi_*$. Since the spectrum for Fig. (1) belongs to the second category of reality condition with $\delta_T^* = 247.9 \text{ GeV}$, no ${}^2\text{BK}$ arises for $\delta_T = 250 \text{ GeV} > \delta_T^*$ as shown in Fig. (1(b)). In any case one can try to fit the endpoints with the segmented maximal endpoint function, Eq. (4) and (5), for given maximal value of $|\delta_T|$, $|\delta_T^{\text{max}}|$ in an event sample, since the $M_{CT2}^{\text{max}}(\chi)$ always increases with $|\delta_T|$. The segmentation point, χ_* of the piecewise fitting function, Eq. (4) and (5) is also a function of α , and overall fitting procedure systematically fits on α without a prior knowledge about χ_* . Then for several $|\delta_T^{\text{max}}|$ values and given χ values, one can extract independent mass constraints, $\alpha(m_Y, m_X, |\delta_T^{\text{max}}|)$ by which the m_Y and m_X can be simultaneously measured.

The M_{CT2} is found to be so sensitive under the Tr. boost of the system that even with moderate values of non-zero δ_T , it can provide good resolving power in discrimination of various transverse boost effects which are usually buried in the large systematic errors of shifted endpoint extraction. The rates of $M_{CT2/T2}^{\text{max}}(\chi)$ shift with respect to a change in δ_T are given as follows :

$$\begin{aligned} & \frac{\partial M_{CT2R/T2R}^{\text{max}}}{\partial |\delta_T|} \\ &= \frac{\alpha E_\chi}{M_{CT2R/T2R}^{\text{max}} E_Y} \left\{ 1 \pm \frac{|\bar{\delta}_T| - \alpha}{E_\chi} \right\} \left\{ 1 \pm \frac{E_Y - \alpha}{E_\chi} \right\}, \end{aligned} \quad (6)$$

for $M_{CT2/T2}$, respectively, with $E_\chi \equiv \sqrt{\chi^2 + (|\bar{\delta}_T| - \alpha)^2}$ and $M_{T2R}^{\text{max}2} = \chi^2 - 2\alpha(|\bar{\delta}_T| - \alpha) + 2\alpha E_\chi$. Here the subscript letter- R denotes the values of $M_{CT2/T2}(\chi)$ for the χ values larger than corresponding kink positions, χ_*/m_X . The shift of the M_{CT2}^{max} is magnified in compared with M_{T2}^{max} as indicated from the flipped signs between the rates of the endpoint shifts in Eq. (6). In particular, the shift can be large by the factor of $O(10)^1$, when the mass difference between M_Y and M_X is small enough so that $|\bar{\delta}_T| > \alpha$ for a moderate value of $|\bar{\delta}_T|$. In Fig. (2(a)) we show the shift of the M_{CT2}^{max} compared with that of M_{T2}^{max} under the effect of non-zero δ_T . We define R as

$$R\left(\frac{|\bar{\delta}_T|}{m_Y}, \frac{m_X}{m_Y}\right) \equiv \frac{M_{CT2}^{\text{max}}(\chi_1, |\bar{\delta}_T| + \Delta) - M_{CT2}^{\text{max}}(\chi_1, |\bar{\delta}_T|)}{M_{T2}^{\text{max}}(\chi_2, |\bar{\delta}_T| + \Delta) - M_{T2}^{\text{max}}(\chi_2, |\bar{\delta}_T|)}.$$

We take $\Delta = m_Y/2$. Also, if $m_X/m_Y = 0.1 - 0.7$, $\chi_1 = 2\chi_*$, where χ_* is calculated with $|\bar{\delta}_T| = |\bar{\delta}_T| + \Delta$, while $\chi_1 = m_X + m_Y/2$ if $m_X/m_Y = 0.8 - 0.9$. Under the transverse boost effect, the magnified shift of $M_{CT2}^{\text{max}}(\chi, \delta_T)$ can be clearly seen depending on the various mass ratios of m_X/m_Y in Fig. (2(a)). If we com-

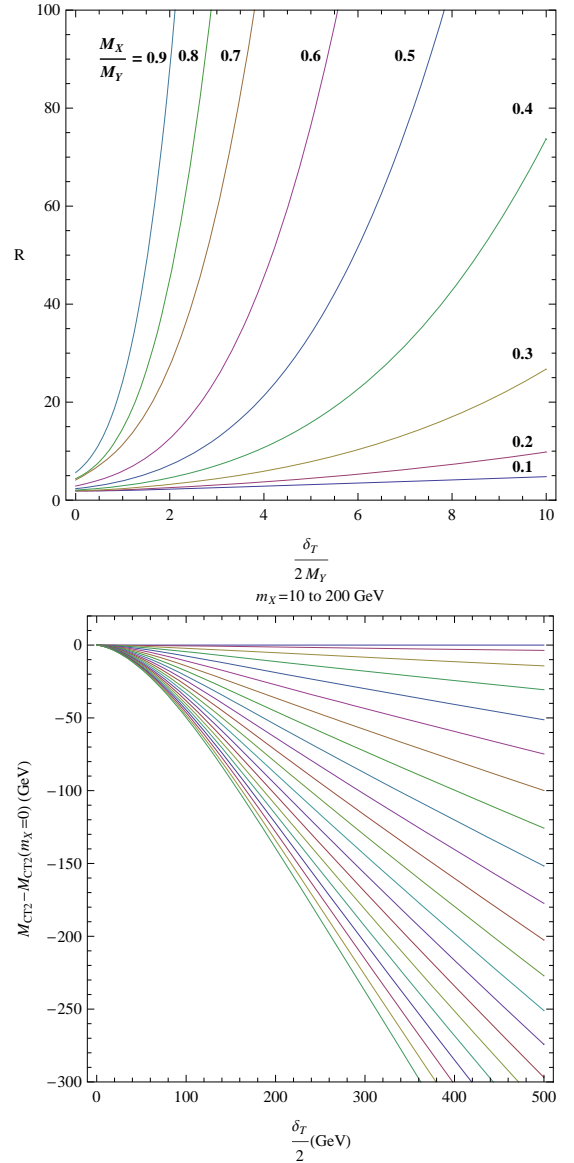


FIG. 2: a) Ratios of δ_T -shift between M_{CT2}^{max} and M_{T2}^{max} with respect to δ_T/M_Y for various mass spectrums, M_X/M_Y . b) δ_T -shift of $M_{CT2}^{\text{max}} - M_{CT2}^{\text{max}}(m_X = 0)$ for $m_X = (10 - 190) \text{ GeV}$ with the $\alpha_0 = 62.4 \text{ GeV}$ and the trial LNP mass, $\chi = \chi_* + 50 \text{ GeV}$.

pare the shifts of the $M_{CT2/T2}^{\text{max}}$ using specific mass spectrums with transverse boost effect, $(m_Y, m_X, |\bar{\delta}_T|, \Delta) = (150, 100, 100, 100)|(500, 100, 100, 100)$, then the shifts of $M_{CT2/T2}^{\text{max}}(\chi)$ are calculated to be $\Delta M_{CT2}^{\text{max}}(\chi = \chi_*) = 73.5|38.4 \text{ GeV}$ while $\Delta M_{T2}^{\text{max}}(\chi = 200 \text{ GeV}) = 12.7|11.6 \text{ GeV}$.

In calculating the R , the optimal choices of $\chi_{1,2}$ for which each of the shifts is maximized and well-measured, are ambiguous. We choose $\chi_1 \sim O(\chi_*)$ because it always provides sizable shift with clean and sharp endpoint structures of the M_{CT2} distributions [8]. A practical choice of χ_2 is also unclear. Indeed, as we take larger value of χ_2 , the denominator of R increases, reducing R down to $O(1)$ in some cases. However, as we

¹ Actually, the sensitivity is not only for the EKC events. The relation (6) holds for all events with general visible transverse momentum smaller than α .

will see in next section, there appear faint long tails near the expected endpoints of the M_{CT2} distributions for large δ_T , making it difficult to measure the endpoints and the shifts. Also, for a given value of δ_T , such an endpoint structure becomes worse as the χ increases over the true value of $\chi = m_X$, while the denominator of R gets rapidly saturated just with $\chi \sim O(m_X) > m_X$. Thus for the sake of both of the endpoint sharpness and the sizable endpoint shift, we choose $\chi_2 - m_X \sim m_Y/2$ so as to fix the separation of χ from the true mass, m_X to be the order of m_X , at least to be $m_X/2$ in Fig. (2(a)).

Fig. (2(b)) displays the δ_T -shift of $M_{CT2}^{\max} - M_{CT2}^{\max}(m_X = 0)$ for various missing LNP masses, $m_X = (10 - 190)$ GeV while the α_0 is fixed by 62.4 GeV and the trial LNP mass, $\chi = \chi_* + 50$ GeV. For $\delta_T = 0$, no mass resolving power is obtained by the endpoint measurement as expected, however, one can see that the δ_T -shift of M_{CT2}^{\max} can be large enough to measure the new particle masses with the resolution of $O(1 - 10)$ GeV for $\delta_T \sim O(10 - 100)$ GeV. It is also enhanced for the large m_X/m_Y case. We fixed the α_0 because it is the basic momentum scale one can observe in detector regardless of the mass spectra.

By projecting events in the $M_{CT2}(\chi \sim O(\chi_*), \delta_T \neq 0)$ basis, one can get a more sharper edged and δ_T -sensitive event distribution. The flipped sign in the definition of the M_{CT2} variable makes the distribution compact with respect to the internal momentum scale of the system, while being much more sensitive for the external boost momentum δ_T , like a rubber ball. This means that one can have a better chance to measure both of the masses with enhanced resolution in probing the boosted kinematic boundaries.

In the following example, we employ the $M_{CT2}(\chi)$ variable for resolving superparticle masses, especially in the events with a pair of $\tilde{\chi}_1^\pm$ decays. It is well-known that one can efficiently select such NP events by imposing the same-sign (SS) dileptonic condition [9]. This signature provides an important discovery channel in establishing SUSY, because the background is small, however, mass measurement in this channel is difficult because of the existence of extra missing ν s and combinatorial SUSY backgrounds of $\tilde{\chi}_1^\pm (\rightarrow \tilde{\nu} + \ell, \tilde{l} + \nu, W + \tilde{\chi}_1^0)$ decays. There exist a few studies [6] on mass measurement in this event topology. We demonstrate that the mass resolving power is significantly enhanced by using the $M_{CT2}^{\max}(\chi)$ under realistic $|\delta_T|$ values of $\tilde{\chi}_1^\pm$ pairs arising from squark/gluino decays.

SUSY example We demonstrate the mass measurement of $\tilde{\chi}_1^\pm$ and $\tilde{\nu}$ for a SUSY benchmark point described in Ref. [7]. In this scenario, 3rd generation sfermions are very heavy and $\tilde{\chi}_1^\pm$ has no branching ratio (BR) to $\tilde{\tau}$ with $\text{BR}(\tilde{\chi}_1^\pm \rightarrow \ell + \tilde{\nu}) = 0.63$ followed by $\tilde{\nu} \rightarrow \tilde{\chi}_1^0 + \nu$. The relevant mass spectrum of the point is $(m_{\tilde{g}}, m_{\tilde{q}}, m_{\tilde{\chi}_1^\pm}, m_{\tilde{\nu}}, m_{\tilde{\chi}_1^0}) = (\sim 720, \sim 635, 231.5, 157.2, 123.3)$ GeV with $\sigma_{tot}^{SUSY} \sim 17$ pb. We calculate $M_{CT2}(\chi)$ for a system of a pair of SS chargino

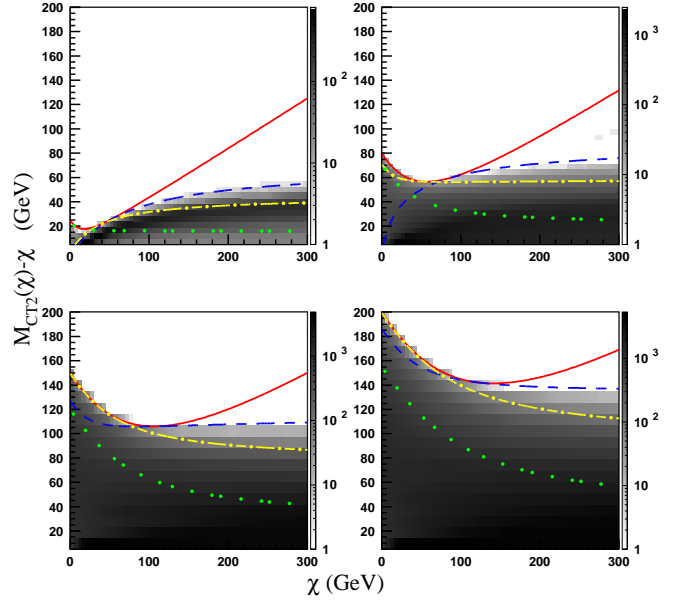


FIG. 3: Contour plots of the SS SUSY dileptonic events surviving the event selection cuts in $M_{CT2}(\chi) - \chi$ vs χ plane for $|\delta_T^{\max}| = (50_{\text{Top-Left}}, 160_{\text{T-Right}}, 300_{\text{Bottom-L}}, 400_{\text{B-R}})$ GeV.

decays, where α_T and β_T are the transverse momenta of leptons from the chargino decays, and the two missing $\tilde{\nu}$'s momenta provide \cancel{E}_T [10]. All of the other jets in the event are taken as the δ_T of the chargino decay system. SUSY events of $70fb^{-1}$ at $\sqrt{s} = 14$ TeV are generated by PYTHIA [11] for this point. The detector simulation is implemented with PGS4 [12].

We select SS dileptonic events with $N(\geq 2)$ -jets + \cancel{E}_T . The event selection cuts are $P_T(\ell_{1,2}) > 20$ GeV, $P_T(jet_{1,2}) > (100, 80)$ GeV, and $\cancel{E}_T > 100$ GeV. After the cuts, the signal to background ratio becomes high and the kinematic endpoints are expected to appear clearly without background from the SM events and neutralino decays [9]. Additionally, we impose a cut on the $|\delta_T|$ value, $|\delta_T| \leq |\delta_T^{\max}|$. For given $|\delta_T^{\max}|$ and χ values, $M_{CT2}^{\max}(\chi)$ (4,5) of the signal events is completely described by two known ($|\delta_T| = |\delta_T^{\max}|/2, \chi$) and two unknown ($m_{\tilde{\chi}_1^\pm}, m_{\tilde{\nu}}$) parameters. Fig. (3) shows the contour histogram of the events which survived the cuts in the $M_{CT2}(\chi) - \chi$ vs χ plane for $|\delta_T^{\max}| = (50_{(a)}, 180_{(b)}, 300_{(c)}, 400_{(d)})$ GeV. The events are populated below the expected endpoints of $M_{CT2}(\chi)$ (4,5). The solid lines show $M_{CT2}^{\max}(\chi)$ (4) for all of the $|\delta_T^{\max}|$ values. The boundaries of the M_{CT2} distributions are well described by the solid lines in the range of $\chi \leq \chi_*(= 53.4_{(a)}, 91.3_{(b)}, 109.3_{(c)}, 120.7_{(d)})$ GeV in Fig. (3). In each plot, we also show three functional lines of $M_{CT2}^{\max}(\chi > \chi_*, |\delta_T^{\max}|)$ (5) for three different mass spectrums, m_Y (Dashed, Dashed-Dotted, Dotted) = $(m_{\tilde{\chi}_1^\pm}, m_{\tilde{\chi}_1^\pm} - 30, m_{\tilde{\chi}_1^\pm} - 60)$ GeV, with the same $m_X = m_{\tilde{\nu}}$ values. The boundary of the $M_{CT2}(\chi, |\delta_T^{\max}|)$ distributions also appear to be well-matched with the expected

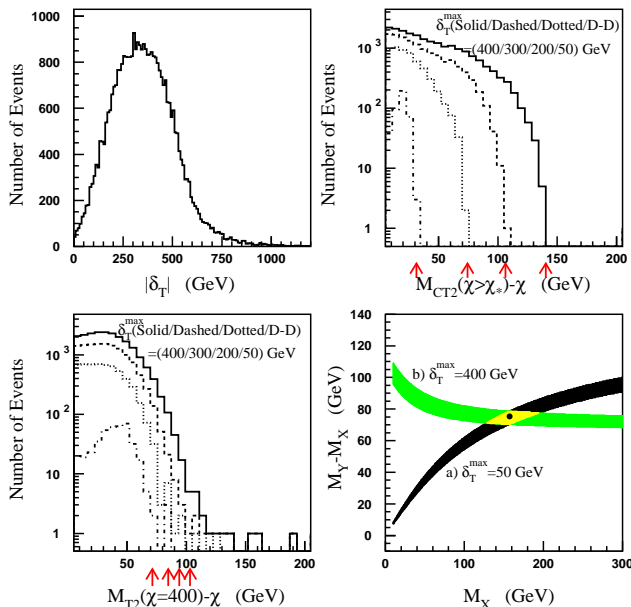


FIG. 4: a)^{T-L} $|\delta_T|$ distribution of the SS dilepton + E_T system surviving the cuts. b)^{T-R} M_{CT2} and c)^{B-L} M_{T2} distributions. d)^{B-R} Consistent mass ranges in $M_Y - M_X$ vs M_X plane.

Dashed-lines for $\chi \geq \chi_*$.

Using the reconstructed $M_{CT2}^{\max}(\chi)$ for different $|\delta_T^{\max}|$ values, we finally attempt to get the consistent range of chargino and sneutrino masses. Fig. (4(a)) shows the $|\delta_T|$ distribution of the SS dilepton + E_T system after the cuts. The event statistics near $|\delta_T| \sim O(100)$ GeV are very rich due to the large boost effect of hard jets from initially produced colored superparticles, and it can be a good testbed for the mass measurement utilizing various transverse boost effects. For different values of $|\delta_T^{\max}| = (400_{\text{Solid}}, 300_{\text{Dashed}}, 200_{\text{Dotted}}, 50_{\text{D-D}})$ GeV cuts, corresponding $M_{CT2}(\chi = \chi_* + \sim 20 \text{ GeV})$ distributions are shown as in Fig. (4(b)). Fig. (4(c)) displays $M_{T2}(\chi = 400 \text{ GeV})$ distributions with the $|\delta_T^{\max}|$ cuts. In both of the plots, red arrows denote the expected endpoints of the $M_{CT2}/M_{T2}(\chi)$ for the given $|\delta_T^{\max}|$ cuts. Then one can clearly see that

1. The endpoint structure of the $M_{CT2}(\chi)$ distribution is statistically cleaner with less pollution [8] and sharper [4] in wide range of $|\delta_T^{\max}|$, compared with $M_{T2}(\chi)$.
2. The M_{CT2} is so sensitive under the transverse boost effect, the shift of M_{CT2}^{\max} with a change of

$|\delta_T^{\max}|$ can be sizable well beyond the uncertainties in endpoint extraction, as well as the number of events contributing to $M_{CT2}(\chi, |\delta_T| > |\delta_T^{\max}|) > M_{CT2}^{\max}(\chi, |\delta_T^{\max}|)$, is much larger than the number of the events with $M_{T2}(\chi, |\delta_T| > |\delta_T^{\max}|) > M_{T2}^{\max}(\chi, |\delta_T^{\max}|)$

Putting all these facts together, we now have a collider variable with which the measurement of Tr. boost-shifted endpoints are experimentally reliable for mass determination under various systematic uncertainties of endpoint extraction.

An error profile function of χ , $\epsilon(\chi) = a \setminus b(\chi - \chi_*) + c$ is assumed in the two regions of ($\chi \leq \chi_* \setminus \chi > \chi_*$), which are likely to be obtained by simple endpoint fitting of $M_{CT2}(\chi, |\delta_T^{\max}|)$ distributions. The coefficients are conservatively set to $(a, b, c) = (2|3, 0.03, 2|3)$ GeV for $|\delta_T^{\max}| = (50|400)$ GeV. Then, for the two $|\delta_T^{\max}|$ values we fit two α values in Eq. (3) and (5), using the parameterized endpoint measurements, $M_{CT2}^{\max}(\chi, |\delta_T^{\max}|) \pm \epsilon(\chi)$ in the range of $0 \leq \chi \leq 300$ GeV, including χ_* which is also a function of α . This is a one-parameter fitting of α for a given $|\delta_T^{\max}|$ value, and the precision of fit result is not much affected by a change of the fit region of χ , as long as it is taken broadly ($0, \chi_* + O(50-100)$ GeV) enough to include the χ_* region. For the parameterized errors, $\alpha \pm \delta\alpha$ values are fitted to be $(69.5|136.5) \pm (3.38|5.14)$ GeV for $|\delta_T^{\max}| = (50|400)$ GeV, with $\chi^2/ndf < 1$. Fig. (4(d)) shows two bands (Green—Black) in $M_Y - M_X$ vs M_X plane, consistent with the fitted α values. The black dot indicates the true mass point and the yellow intersection region is the 1σ range of the mass measurement using the $M_{CT2}^{\max}(\chi)$ data for two different $|\delta_T^{\max}|$ cuts.

Discussion In this paper we study the $M_{CT2}(\chi)$ endpoint of a system containing a pair of single step decays, which is expected to be the simplest non-trivial new physics event topology. The M_{CT2} magnifies the transverse boost effect on the system, while keeping its endpoint structure clean and sharp. Thus, measuring M_{CT2}^{\max} for different $|\delta_T|$ values can provide us with reliable resolving power to determine both masses of mother and missing daughter particles only using moderate transverse boost momentum of the system of our interest. With realistic δ_T profiles of mSUGRA like events, we demonstrate simultaneous mass measurement of $\tilde{\chi}_1^\pm$ and $\tilde{\nu}$ in SS dileptonic decay channel, where $\tilde{\chi}_1^\pm \rightarrow \tilde{\nu} + \ell$. The technique also works for a single mother particle decay system with non-zero transverse momentum.

This work was supported by World Premier International Center Initiative (WPI Program), MEXT, Japan.

[1] W. S. Cho, K. Choi, Y. G. Kim and C. B. Park, Phys. Rev. Lett. **100**, 171801 (2008); W. S. Cho, K. Choi, Y. G. Kim and C. B. Park, J. High Energy Phys. **02**, 035

(2008).

[2] B. Gripaios, J. High Energy Phys. **02**, 053 (2008); A. Barr, B. Gripaios and C. Lester, J. High Energy Phys.

- 02**, 014 (2008), *J. High Energy Phys.* **11**, 096 (2009); M. Burns, K. Kong, K. Matchev and M. Park, *J. High Energy Phys.* **03**, 143 (2009).
- [3] C. Lester and D. Summers, *Phys. Lett. B* **463**, 99 (1999); A. Barr, C. Lester and P. Stephens, *J. Phys.* **G29** (2003) 2343.
- [4] W. S. Cho, J. E. Kim and J. H. Kim *Phys. Rev. D* **81**, 095010 (2010); A. Barr, C. Gwenlan, C. Lester, and C. Young, *Phys. Rev. D* **83**, 118701 (2011).
- [5] R. Tovey, *J. High Energy Phys.* **04**, 034 (2008); M. Serna, *J. High Energy Phys.* **06**, 004 (2008); G. Polesello and D. R. Tovey, *J. High Energy Phys.* **03**, 030 (2010).
- [6] K. T. Matchev, F. Moortgat, L. Pape and M. Park, *Phys. Rev. D* **82**, 077701 (2010); T. Cohen, E. Kuflik and K. Zurek, *JHEP* **1011**, 008 (2010); P. Konar, K. Kong, K. T. Matchev and M. Park, *Phys. Rev. Lett.* **105**, 051802 (2010)
- [7] S. K. Mandal, M. Nojiri, M. Sudano, T. T. Yanagida, *J. High Energy Phys.* **01**, 131 (2011);
- [8] W. S. Cho, et al. work in progress.
- [9] The ATLAS Collaboration, CERN-OPEN-2008-020
- [10] The other decay channel, $\tilde{\chi}_1^\pm \rightarrow \tilde{l} + \nu_\ell$, is also open, however it does not give the maximum of $M_{CT2}(\chi)$ in this spectrum [8].
- [11] T. Sjostrand, S. Mrenna, and P. Skands, *J. High Energy Phys.* **05**, 026 (2006).
- [12] PGS4, J. Conway, <http://www.physics.ucdavis.edu/~conway/research/software/pgs/pgs4-general.htm>.